

## CFD Simulation for Flow Control Devices of Helicopter Rotor

**Mr. Shiva Shanker**  
Associate Professor  
MLRIT  
Dundigal, Hyderabad.

**Rajesh. K**  
M.Tech Student,  
MLRITM  
Dundigal, Hyderabad.

### ABSTRACT

*In this project simulation of flow control devices and the assessment of their impact on the aerodynamic performance of helicopter rotors at different angle of attack and Mach numbers is carried out. Computation has carried out using commercial CFD package CFX. Computational results show that a separation of flow appears at 8deg, 12deg, 18deg angles of attack and Mach number (M) 0.3. For controlling the separation special boundary condition has been applied. A jet is created on the aerofoil at 75% of the chord length. By blowing air the flow separation can be controlled and this enhances for the improvement of aerodynamic performance of the rotor blade.*

**Key Words:** Helicopter rotors, CFD package, CFX etc.

### INTRODUCTION

#### SCOPE OF THE PROJECT

The current approach is based on performing 3D CFD calculations using the CFD solver CFX. Several flow control devices have been assessed including trailing edge flaps, leading edge slats, Gurney flaps, air jet vortex generators as well as synthetic jets. Having obtained some understanding of the effect of each flow control device on the aerodynamics of the rotor, 3D CFD computations were undertaken for full rotor blades with blowing jets control devices deployed to delay flow separation. The location of jet has varied at various angles of attack to improve aerodynamic performance of the rotor.

At the selected conditions the jet is altering the properties of part of the boundary layer in a small region downstream of its location. This is the small-

scale problem to be resolved. The size of the air jet is almost half of the thickness of the boundary layer and thousand times smaller than the span of a rotor where it could be deployed.

From the computational results we can decide about the air jet placement that has to be applied to the flow. This kind of computational work can be performed commercially available CFD packages with less effort and cost. Hence different strategies can be tested to improve the flow control devices.

### PROBLEM DEFINITION

The numerical simulation of the various flow control devices varies in difficulty and several open issues remain regarding the applicability of CFD for such simulations. The main problem encountered is the presence in the simulation domain of multiple temporal and spatial scales. This, however, is not a new problem in CFD.

In fact, the step from inviscid simulations of flows around aerofoils using Euler's equations to Navier-Stokes simulations where the boundary layers had to be resolved is one of the first times problems with differences in flow scales have encountered. The resolution of the flow near the shock is another good example. No CFD solver based on the Navier-Stokes equations in industrial practice is actually fully resolving the structure of shocks.

Although modern CFD solvers resolve the boundary layers, laminar and turbulent ones, to good accuracy, the effect of the shock on the flow is actually modeled by changing the order of the employed discretisation scheme and applying special limiters.

## OBJECTIVES OF THE PROJECT

The objective of project is to simulate the flow control device of helicopter rotor blade using CFD SOLVER software.

The baseline CFD solver is described. For this work the following extensions where necessary. A technique for modeling jet blower along with special boundary conditions.

Simulation of flow over an airfoil at different angles of attack has been reported for 0.3 Mach number. Computation has been carried out using CFD packages.

Design and analysis of 3D comparison with reference values.

## LIMITATIONS OF THE PROJECT

There are limitations with this approach though the obtained results indicate that it can be used for analysis of devices like vortex generators and air-jet blowers on rotor blades. The key idea is to embed pressurized jet in the flow with appropriate circulation where vortices due to flow separation are to be avoided. This can be done by adding momentum and energy sources to the conservation laws used in CFD. The sources are activated around jet blower and switched off in the majority of the field.

The limitations of linear eddy-viscosity models that may influence the simulation of flow control devices are (i) the excessive amount of eddy viscosity produced in jet-core regions, (ii) the inability to predict secondary flows normal to the dominant flow direction, and (iii) the overproduction of eddy viscosity near stagnation points. All three issues are important since devices like flaps and slats result in extra stagnant flow regions and devices like vortex generators produce vortices which travel in the streamwise direction. The current technique is based on a very simple idea that combines a rigid movement of the whole CFD grid followed by grid to jet. The quality of the deformed grid was found to depend on the initial CFD mesh.

## DESIGN

The helicopter rotor is powered by the engine, through the transmission, to the rotating mast. The mast is a cylindrical metal shaft that extends upward from and is driven by the transmission. At the top of the mast is the attachment point for the rotor blades called the hub. The rotor blades are then attached to the hub. Main rotor systems are classified according to how the main rotor blades are attached and move relative to the main rotor hub. There are three basic classifications: rigid, semirigid, or fully articulated, although some modern rotor systems use an engineered combination of these classifications. The rotors are designed to operate in a narrow range of RPM.

Unlike the small diameter fans used in turbofan jet engines, the main rotor on a helicopter has a large diameter that lets it accelerate a large volume of air. This permits a lower downwash velocity for a given amount of thrust. As it is more efficient at low speeds to accelerate a large amount of air by a small degree than a small amount of air by a large degree, a low disc loading (thrust per disc area) greatly increases the aircraft's energy efficiency and this reduces the fuel use and permits reasonable range.

## METHODOLOGY

### GEOMETRY MAKING

### SOFTWARE USED: ANSYS ICEM CFD

We used NACA 0015 aerofoil, with the following co-ordinates for reference:

1.0000	0.00158	0	1.0000	0.00158	10
0.9500	0.01008	0	0.9500	0.01008	10
0.9000	0.01810	0	0.9000	0.01810	10
0.8000	0.03279	0	0.8000	0.03279	10
0.7000	0.04580	0	0.7000	0.04580	10
0.6000	0.05704	0	0.6000	0.05704	10
0.5000	0.06617	0	0.5000	0.06617	10
0.4000	0.07254	0	0.4000	0.07254	10
0.3000	0.07502	0	0.3000	0.07502	10
0.2500	0.07427	0	0.2500	0.07427	10
0.2000	0.07172	0	0.2000	0.07172	10
0.1500	0.06682	0	0.1500	0.06682	10
0.1000	0.05853	0	0.1000	0.05853	10
0.0750	0.05250	0	0.0750	0.05250	10
0.0500	0.04443	0	0.0500	0.04443	10
0.0250	0.03268	0	0.0250	0.03268	10
0.0125	0.02367	0	0.0125	0.02367	10
0.0000	0.00000	0	0.0000	0.00000	10
0.0125	-0.02367	0	0.0125	-0.02367	10
0.0250	-0.03268	0	0.0250	-0.03268	10
0.0500	-0.04443	0	0.0500	-0.04443	10
0.0750	-0.05250	0	0.0750	-0.05250	10
0.1000	-0.05853	0	0.1000	-0.05853	10
0.1500	-0.06682	0	0.1500	-0.06682	10

**TABLE NO: 1 REFERENCE POINTS OF NACA 0015 AIRFOIL**

With the help of the above co-ordinates, the points were plotted as follows.

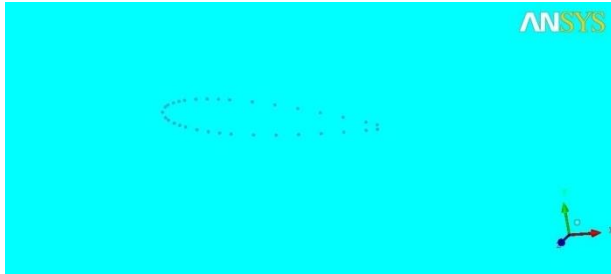


**Fig: 5 AEROFOIL POINTS**

Once the points were joint, an approximate (10m) wingspan was given.

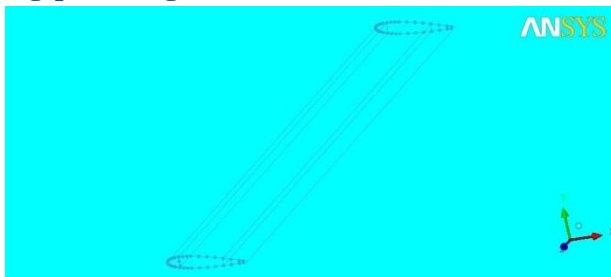


**Fig: 6 JOINING OF AEROFOIL**

Wire frame of the aerofoil is now surfaced.

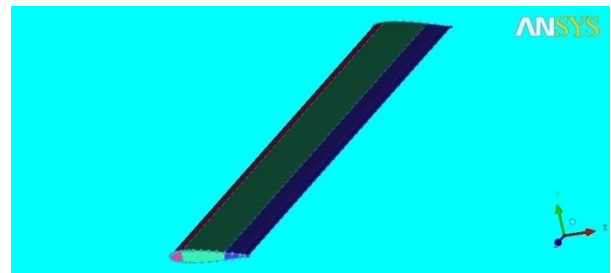


**FIG: 7 SURFACE CREATION OF AEROFOIL**

The aerofoil is placed in a rectangular test section with approximate values.

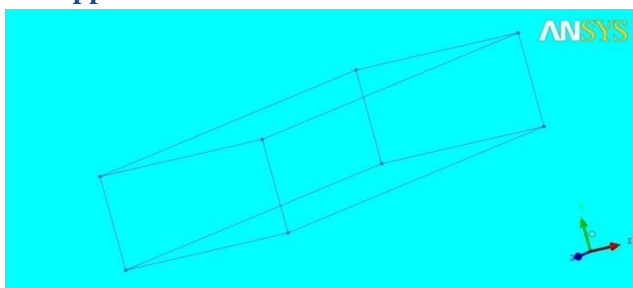


**FIG: 8 CREATION OF TEST SECTION  
(DOMAIN)**

The medium surrounding the aerofoil in the test section is taken as Air.

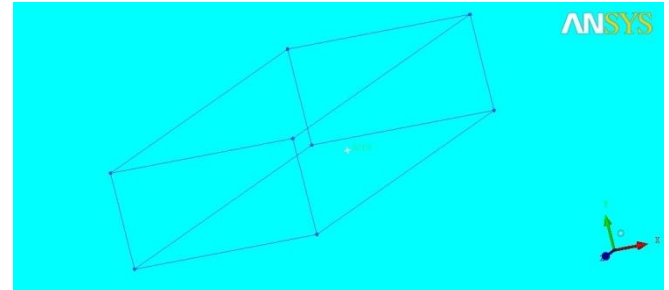


**FIG: 9 DOMAIN WITH BODY**

The test section consisting of INLET, OUTLET, SIDES and WALLS are surfaced.

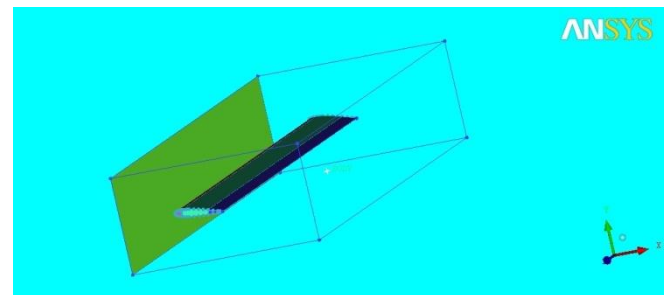


**FIG: 10 SURFACING OF DOMAIN INLET**

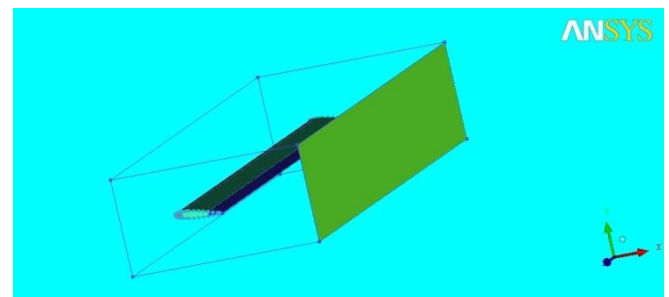


**FIG: 11 SURFACING OF DOMAIN OUTLET**

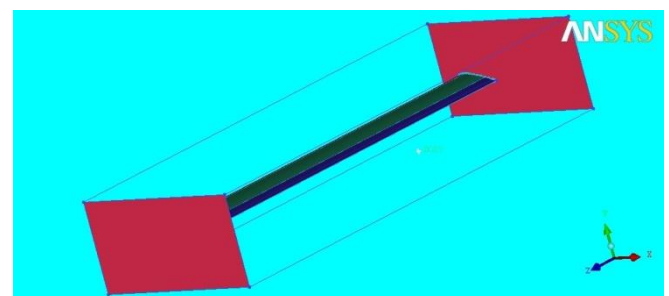


**FIG: 12 SURFACING OF DOMAIN SIDES**

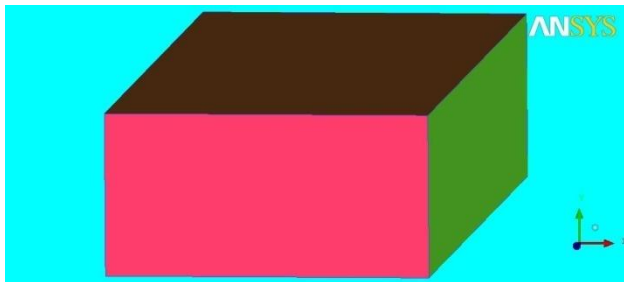


**FIG: 13 SURFACE OF TEST SECTION**

Open view of the test section with the aerofoil and fluid.

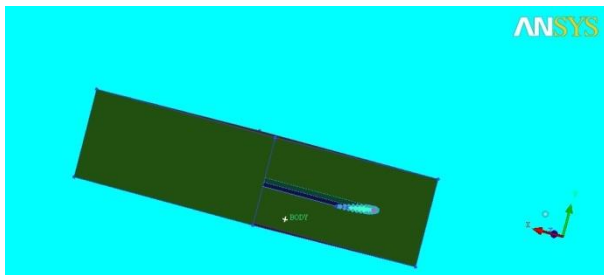


**FIG: 14 OPEN VIEW OF TST SECTION**

At the 75% of the chord length the blower (flow control device) is projected i.e on the trailing edge. The approximate values are taken to create the blower.

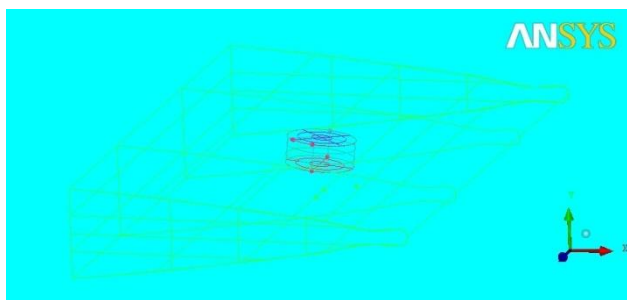


**FIG: 15 PROJECTION OF JET BLOWER**

Below we can see the aerofoil and blower.

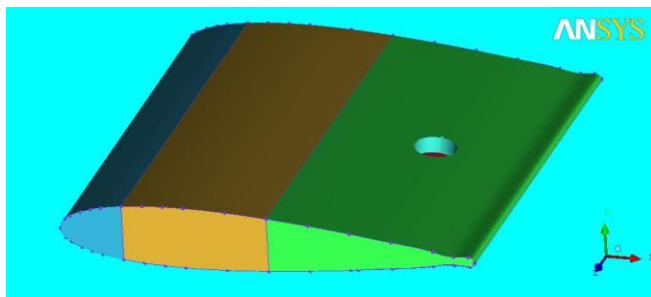


**FIG: 16 AEROFOIL AND JET BLOWER**

**ANALYSIS**

**SOFTWARE USED: ANSYS CFX**

**PRE-PROCESSING:**

**Physics Report**

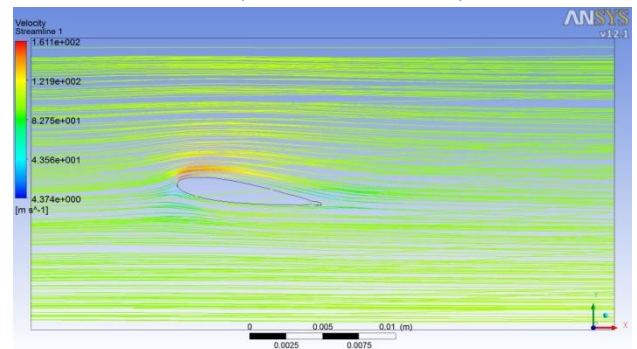
**Domain Physics for 8 deg\_001**

Domain - Default Domain	
Type	Fluid
Location	BODY
Materials	
Air at 25 C	
Fluid Definition	Material Library
Morphology	Continuous Fluid
Settings	
Buoyancy Model	Non Buoyant
Domain Motion	Stationary
Reference Pressure	1.0000e+00 [atm]
Heat Transfer Model	Isothermal
Fluid Temperature	2.5000e+01 [C]
Turbulence Model	k epsilon
Turbulent Wall Functions	Scalable

**TABLE: 3 PHYSICAL REPORT OF DOMAIN**

**RESULTS**

**CASE 1 – ANGLE OF ATTACK 8 deg, VELOCITY 99m/s(WITHOUT JET)**



**FIG; 24 FLOW SEPARATIONS ON AIRFOIL**

**Pressure contour at 8 deg, velocity 99m/s**

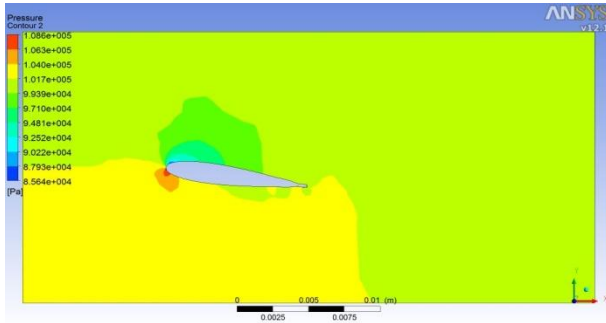


**FIG: 25 PRESSURE CONTOUR AT 8 DEG**

**Pressure contour at 12 deg, velocity 99m/s**

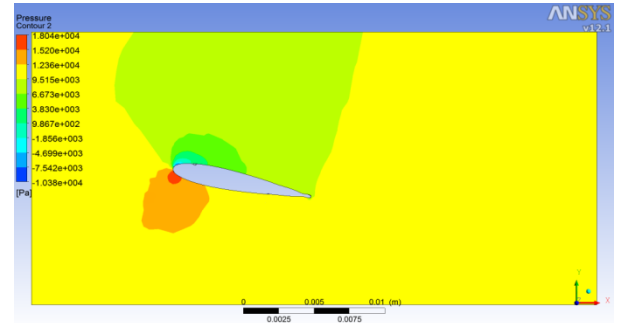


**FIG:29 PRESSURE CONTOUR AT 12 DEG**

**Velocity contour at 8 deg, velocity 99m/s**

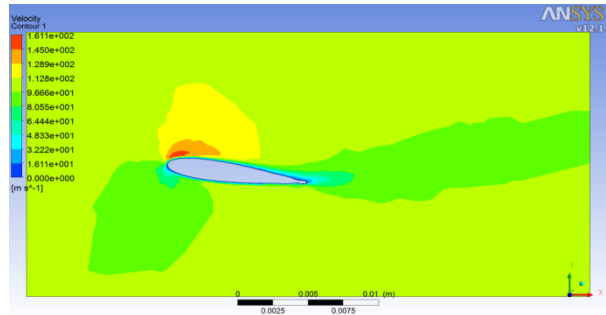


**FIG: 26 VELOCITY CONTOUR AT 8 DEG**

**Velocity contour at 12 deg, velocity 99m/s**

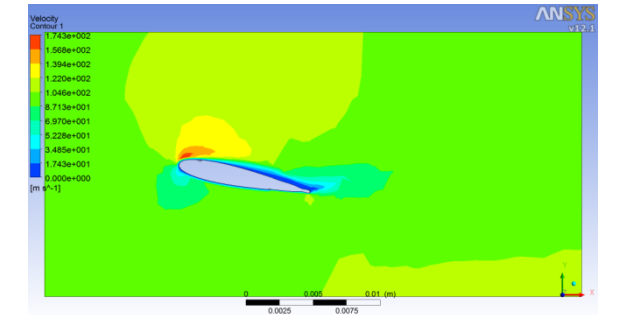


**FIG:30 VELOCITY CONTOUR AT 12 DEG**

**CASE 2- ANGLE OF ATTACK 12 deg,  
 VELOCITY 99m/s(WITHOUT JET)**

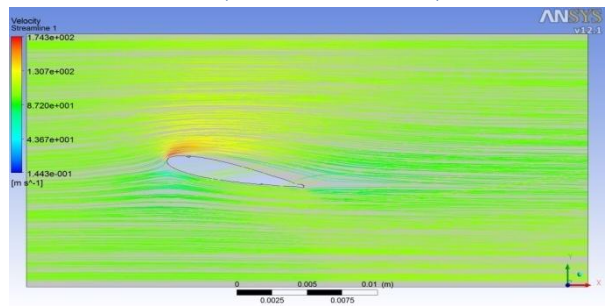


**FIG: 27 FLOW SEPARATIONS AT 12 DEG**

**CASE 3-ANGLE OF ATTACK 18 deg,  
 VELOCITY 99m/s, (WITHOUT JET)**

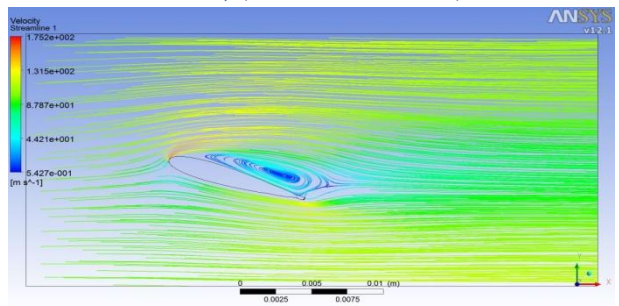


**FIG:31 FLOW SEPARATIONS AT 18 DEG**

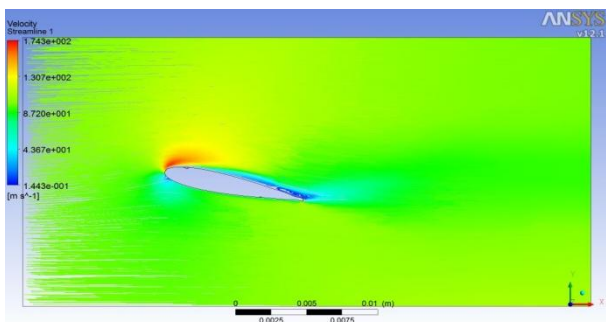


**FIG: 28 VELOCITY STREAM LINES AT 12 DEG**

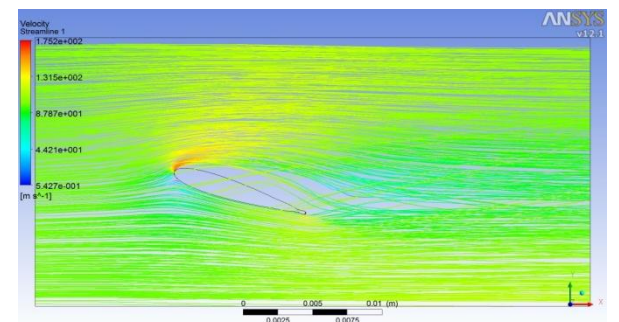


**FIG:32 VELOCITY STREAM LINES AT 18 DEG**

**Pressure contour at 18 deg, velocity 99m/s**

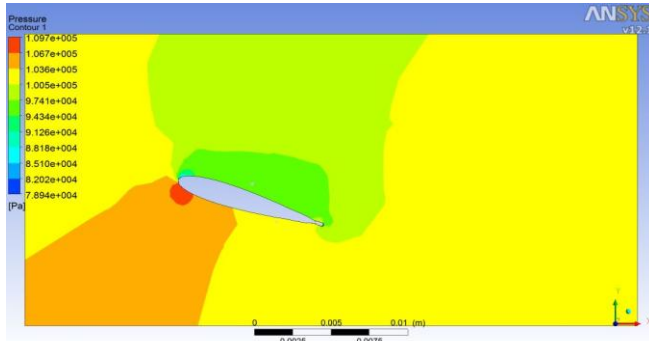


**FIG: 33 PRESSURE CONTOUR AT 18 DEG**

**Velocity contour at 18 deg, velocity 99m/s**

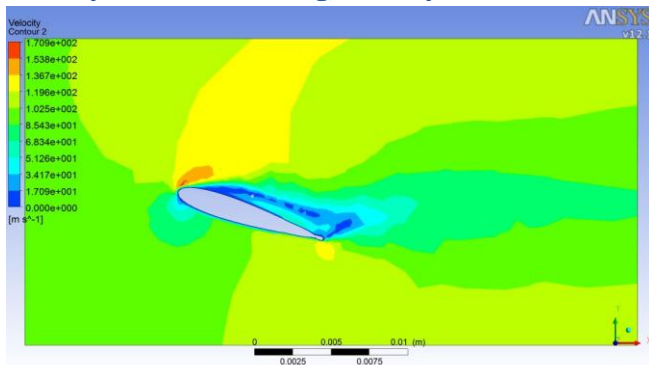


**FIG:34 VELOCITY CONTOUR AT 18 DEG**

### CONCLUSION & FUTURE SCOPE OF WORK

The aerodynamic performance of the rotor blade can be increased with the use of flow control devices at higher angles of attack. Considering the above case analysis we can successfully attain the delay of flow separation over the boundary layer of the airfoil. Hence increment in the aerodynamic performances of the rotor blades.

The current approach is based on performing 3D CFD calculations using the CFD solver CFX. Several flow control devices have been assessed including trailing edge flaps, leading edge slats, Gurney flaps, air jet vortex generators as well as synthetic jets. Having obtained some understanding of the effect of each flow control device on the aerodynamics of the rotor, 3D CFD computations were undertaken for full rotor blades with blowing jets control devices deployed to delay flow separation. The location of jet has varied at

various angles of attack to improve aerodynamic performance of the rotor.

At the selected conditions the jet is altering the properties of part of the boundary layer in a small region downstream of its location. This is the small-scale problem to be resolved. The size of the air jet is almost half of the thickness of the boundary layer and thousand times smaller than the span of a rotor where it could be deployed.

From the computational results we can decide about the air jet placement that has to be applied to the flow. This kind of computational work can be performed commercially available CFD packages with less effort and cost. Hence different strategies can be tested to improve the flow control devices.

### References

1. Unsteady Aerodynamics Experiment Phase VI: Wind Tunnel Test Configurations and Available Data Campaigns M.M. Hand, D.A. Simms, L.J. Fingersh, D.W. Jager, J.R. Cotrell, S. Schreck, and S.M. Larwood December 2001 • NREL/TP-500-29955
2. CFD Calculations of S809 Aerodynamic characteristics by Walter P. Wolfe and Stuart S. Ochs of AIAA-97-0973
3. Hau, E. Wind Turbines, Fundamentals, Technologies, Application, Economics, 2nd ed.; Springer: Berlin, Germany, 2006.
4. Dominy, R.; Lunt, P.; Bickerdyke, A.; Dominy, J. Self-starting capability of a darrieus turbine. Proc. Inst. Mech. Eng. Part A J. Power Energy 2007, 221, 111–120.
5. Holdsworth, B. Green Light for Unique NOVA Offshore Wind Turbine, 2009. Available online: <http://www.reinforcedplastics.com> (accessed on 8 May 2012).



6. Gasch, R.; Twele, J. Wind Power Plants; Solarpraxis: Berlin, Germany, 2002.
7. Gorban, A.N.; Gorlov, A.M.; Silantsev, V.M. Limits of the turbine efficiency for free fluid flow.
8. J. Energy Resour. Technol. Trans. ASME 2001, 123, 311–317.
9. Burton, T. Wind Energy Handbook; John Wiley & Sons Ltd.: Chichester, UK, 2011.
10. Hull, D.G. Fundamentals of Airplane Flight Mechanics; Springer: Berlin, Germany, 2007.
11. INTERNATIONAL JOURNAL OF ENERGY AND ENVIRONMENT Volume 4, Issue 5, 2013 pp.825-834 CFD analysis of horizontal axis wind turbine blade for optimum value of power.